Multi-population model of a microbial electrolysis cell
Pinto, R. P.; Srinivasan, B.; Escapa, A.; Tartakovsky, B.

National Research Council Canada   Conseil national de recherches Canada

Canada

Multi-Population Model of a Microbial Electrolysis Cell

R. P. Pinto,[†,‡] B. Srinivasan,[‡] A. Escapa,[§] and B. Tartakovsky[*,†,‡]

[†]Biotechnology Research Institute, National Research Council of Canada, 6100 Royalmount Avenue, Montreal, QC, Canada H4P 2R2
[‡]Departement de Génie Chimique, École Polytechnique Montréal, C.P.6079 Succ., Centre-Ville Montreal, QC, Canada H3C 3A7
[§]Chemical Engineering Department, University of León, IRENA-ESTA Avda. de Portugal 41, León 24071, Spain

Ⓢ *Supporting Information*

ABSTRACT: This work presents a multi-population dynamic model of a microbial electrolysis cell (MEC). The model describes the growth and metabolic activity of fermentative, electricigenic, methanogenic acetoclastic, and methanogenic hydrogenophilic microorganisms and is capable of simulating hydrogen production in a MEC fed with complex organic matter, such as wastewater. The model parameters were estimated with the experimental results obtained in continuous flow MECs fed with acetate or synthetic wastewater. Following successful model validation with an independent data set, the model was used to analyze and discuss the influence of applied voltage and organic load on hydrogen production and COD removal.
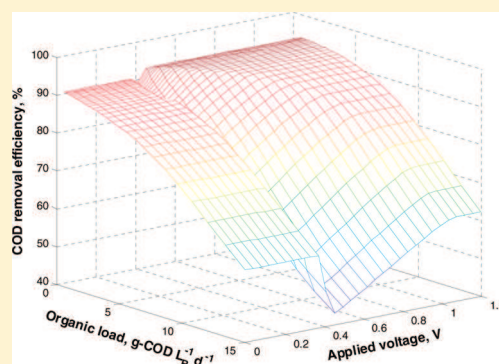
■ INTRODUCTION

Organic matter conversion to hydrogen in a microbial electrolysis cell (MEC) offers a number of advantages in comparison to H$_2$ production by water electrolysis, which requires a significant energy input, and to fermentative H$_2$ production, which has a limited yield of not more than 25%.[1−3] Intensive MEC research in recent years has led to significant improvements in the volumetric rate of H$_2$ production, cathode materials, MEC design, and operating conditions, yet the overall performance remains relatively low.[2,4] One solution for the complex problems posed by MEC research is to develop a mathematical model that can describe the dynamics of chemical oxygen demand (COD) consumption and H$_2$ production in a MEC. This model can then be used to optimize the MEC operational parameters and design, thus facilitating the development of a full-scale MEC-based wastewater treatment process. Although several microbial fuel cell (MFC) models have been developed[5−9] and an anodic compartment model has been recently presented,[10] to our best knowledge a MEC model capable of simulating H$_2$ production from complex organic matter has not yet been reported. However, MFC models that can describe the competition between electricigenic and methanogenic microorganisms for acetate have already been presented.[5,7,11] The anaerobic degradation process has also been extensively studied and modeled (e.g., 12−14).

This work presents a simple dynamic model of a MEC developed with the objective to simulate H$_2$ production from wastewater for process design, optimization, and control applications. Furthermore, the model application is illustrated by analyzing the influence of the substrate feed rate (organic load) and applied voltage on COD removal and H$_2$ production.

■ MATERIALS AND METHODS

Analytical Methods. Chemical oxygen demand of synthetic wastewater (sWW) was estimated according to Standard Methods.[15] Both total COD (tCOD) and soluble COD (sCOD) values were analyzed. Acetate, propionate, and butyrate were analyzed using a gas chromatograph. The total concentration of volatile fatty acids (VFAs) was calculated with respect to the COD equivalent of each component. Gas production in the MEC anodic and cathodic chambers was measured online using glass U-tube bubble counters interfaced with a data acquisition system. The gas composition was measured using a gas chromatograph. A detailed description of all analytical methods used in the study can be found in Tartakovsky et al.[16]

MEC Design, Operation, and Characterization. Three membraneless MECs (MEC-1, MEC-2, and MEC-3) with 50-mL anodic and H$_2$-collection compartments were constructed from nylon plates. The anodes were made of 5-mm-thick carbon felt measuring 10 cm × 5 cm (SGL Group, Wiesbaden, Germany). Gas diffusion cathodes with a Ni load of 0.2−0.3 mg cm^{-2} were used in all MECs and prepared as described in Manuel et al.[17] The electrodes were separated by a J-cloth (Associated Brands, Mississauga, Canada) with a thickness of about 0.7 mm. An external recirculation loop was installed for improved mixing of the anodic liquid. The anode compartment temperature and

pH were maintained at 30 °C and 7, respectively, by JCR-33A temperature controller (Shinko Technos Co., Ltd., Osaka, Japan) and PHCN-410 pH controller (Omega Engineering, Stamford CT).

Each MEC was inoculated with 5 mL of anaerobic sludge with volatile suspended solids (VSS) of approximately 40–50 g L^{-1} (Lassonde Inc., Rougemont, QC, Canada) and 20 mL of effluent from an existing acetate-fed MEC. The stock solution of acetate-based feed was composed of (in g L^{-1}) yeast extract (0.8), NH$_4$Cl (18.7), KCl (148.1), K$_2$HPO$_4$ (64.0), and KH$_2$PO$_4$ (40.7). The amount of sodium acetate varied from 20 to 80 g L^{-1} to obtain the desired concentration of carbon source. The stock solution of sWW was composed of (in g L^{-1}) pepticase (50), beef extract (50), yeast extract (30), NH$_4$HCO$_3$ (17), K$_2$HPO$_4$ (1.75), KH$_2$PO$_4$ (1.5).

MEC-1, MEC-2, and MEC-3 were operated at average flow rates of 200, 75, and 60 mL d^{-1}, respectively. The acetate-fed MEC-1 was operated at three influent concentrations of 1000, 1500, and 1900 mg-COD L^{-1}. The sWW-fed MEC-2 was also operated at three influent concentrations of 2500, 4900, and 9000 mg-COD L^{-1}. Finally, sWW-fed MEC-3 was operated at two influent concentrations of 550 and 6200 mg-COD L^{-1}.

The electrical load of each MEC was controlled individually by an adjustable DC power supply (IF40GU, Kenwood, Japan), used to maintain voltage at a preset value, typically between 0.8 and 1.0 V. Voltage scans were carried out by stepwise decreasing the applied voltage from 1.2 to 0.2 V, in 0.2 V steps. Once the voltage setting was changed, a 10-min interval was allowed for voltage and current stabilization, then the current was measured using a multimeter (Fluke 189, Fluke Corp., Everett, WA). The MEC internal resistance (i.e., the sum of the charge transfer resistances and the solution resistance) was estimated using the linear interpolation of the voltage scan in the region of constant voltage drop, $E_{applied} = a_0 + a_1 I_{MEC}$, where $E_{applied}$ is the MEC applied voltage (V), I_{MEC} is the MEC current (A), and a_0, a_1 are the regression coefficients.

Numerical Methods and Calculations. The integration of model equations was performed in MATLAB (version 7.6, The Mathworks Inc., Natick, MA). Model parameters were estimated by minimizing the following objective function:

$$F_{obj} = \sum_{i=1}^{m} \frac{w_i}{n_i} \left(\sum_{j=1}^{n_i} \left(\overline{y}_{j,i}^{exp} - \overline{y}_{j,i}^{sim} \right)^2 \right) \quad (1)$$

where $\overline{y}_{j,i}^{exp}$ and $\overline{y}_{j,i}^{sim}$ are the normalized experimental and simulated values of the i-th state variable, at j-th sampling time, respectively; w_i is the weight constant of the i-th state variable; n_i is the number of measurements (samples) of the i-th state variable; and m is the number of measurable state variables. The measurable variables included sCOD and total VFA concentrations, gas (CH$_4$ and H$_2$) flow and composition in the H$_2$-collection and anode compartments, and current, hence $m = 6$.

To estimate the selected model parameters, the objective function defined in eq 1 was minimized using the Nelder–Mead simplex algorithm[18] implemented in the FMINSEARCH subroutine of the MATLAB Optimization Toolbox.

Model outputs were compared with experimental results using the calculations of the adjusted coefficient of determination (R^2):

$$R^2 = 1 - \frac{1}{n_i} \sum_{j=1}^{n_i} \left(\frac{\overline{y}_j^{exp} - \overline{y}_j^{sim}}{\max(\overline{y}_j^{exp}, \overline{y}_j^{sim})} \right)^2 \quad (2)$$
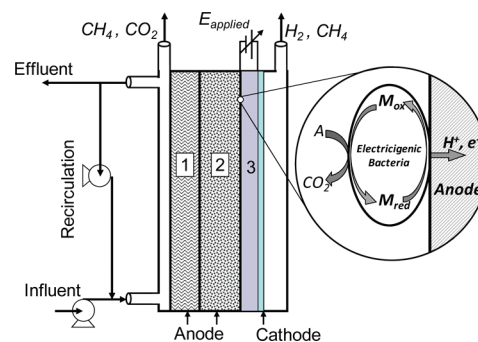

Figure 1. Simplified diagram of a continuous-flow MEC with three biofilm layers. Layer 1 represents the outer anodic biofilm, containing fermentative and acetoclastic methanogenic microorganisms; layer 2 represents the inner biofilm, occupied by electricigenic and methanogenic (acetoclastic) microorganisms; and layer 3 represents the cathode biofilm populated by hydrogenotrophic methanogenic microorganisms. The conceptual acetate conversion in the anodic layer 2 by electricigenic microorganisms is shown in detail. M_{red} and M_{ox} denote reduced and oxidized forms of an intracellular mediator, respectively.

■ MODEL FORMULATION

The main objective of the model is to simulate H$_2$ production from wastewater in a simple, easily identifiable dynamic model, which provides a fast convergence numerical solution and can be conveniently used in process design, control, and optimization. The model equations presented here are based on the two-population MFC model developed by Pinto et al[5] and on the anaerobic digestion model proposed by Bernard et al.[12]

We assumed that the anaerobic degradation of wastewater in the anodic compartment of a MEC can be described by a single hydrolysis and fermentation step of complex organic matter conversion to acetate.[12] Thus, all VFAs are represented by acetate, which is a significant simplification of the complexity of the multistep anaerobic digestion process.[19] This modeling simplification has been demonstrated to be sufficient for an acceptable description of the methane formation dynamics in anaerobic reactors.[12,14,20] Furthermore, the conversion of organic substrate into H$_2$ was considered to be negligible. Acetate is assumed to be consumed by both acetoclastic methanogenic and electricigenic microorganisms.[5] Finally, the model accounts for H$_2$ consumption by hydrogenotrophic methanogens.[21,22]

The MECs used for the experiments employed a three-dimensional carbon felt anode, which occupied most of the anode compartment and offered a good support for the formation of an anaerobic biofilm.[23] Due to the high porosity of the anode and considerably high recirculation rates, we assumed homogeneous distribution of the carbon source and the degradation products throughout the anode. To avoid the use of a distributed parameter model to describe carbon source and product distribution within the biofilm, the model was further simplified by assuming a layered biofilm structure, as proposed by Rauch et al.[24] and using biofilm retention constants[5] in the biomass material balances. The existence of three biofilm layers was considered, as shown in Figure 1. The outer, biofilm layer (Layer 1) was assumed to contain fermentative microorganisms converting wastewater to acetate, and acetoclastic methanogens converting acetate to methane. An inner biofilm, Layer 2, was assumed to contain the electricigenic and acetoclastic methanogenic microorganisms. Finally, the abundance of H$_2$ in a close

proximity to the cathode was assumed to result in the existence of the third biofilm layer adjacent to the cathode and entirely populated by hydrogenotrophic methanogens (Layer 3 in Figure 1).

Other simplifying assumptions included ideal mixing in the anodic compartment, the existence of a constant pool of intracellular electron transfer mediator in electricigenic microorganisms, and the absence of biomass growth in the anodic liquid. Also, temperature and pH were considered fully controlled and maintained at constant levels.

Stoichiometric Equations and Material Balances. Organic substrate transformation to acetate by the fermentative microorganisms (x_f) is assumed to occur in a single step. Such transformation can be illustrated by the conversion of glucose into acetate ($C_6H_{12}O_6 \rightarrow 3C_2H_4O_2$), or in a general form:

$$S \rightarrow nA \qquad (3)$$

where S is the organic substrate concentration (e.g., COD content of wastewater), A is the acetate ($C_2H_4O_2$) concentration, and n is the stoichiometric coefficient.

Acetate consumption by the electricigenic microorganisms (x_e) is described as

$$C_2H_4O_2 + 2H_2O + 4M_{ox} \rightarrow 4M_{red} + 2CO_2 \qquad (4)$$

$$4M_{red} \rightarrow 4M_{ox} + 8e^- + 8H^+ \qquad (5)$$
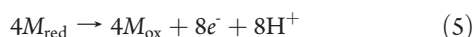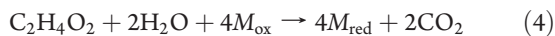
where M_{red} and M_{ox} are the reduced and oxidized forms, respectively, of the intracellular mediator used by the electricigenic microorganisms.

Acetate consumption by the acetoclastic methanogenic microorganisms (x_m), which results in methane and carbon dioxide formation in biofilm Layer 1 and 2 (Figure 1) is described as

$$C_2H_4O_2 \rightarrow CH_4 + CO_2 \qquad (6)$$

Hydrogen consumption by the hydrogenotrophic methanogenic microorganisms (x_h) is described as

$$CO_2 + 4H_2 \rightarrow CH_4 + 2H_2O \qquad (7)$$
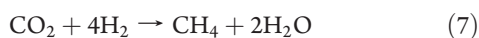
For a continuous flow MEC with equal influent and effluent flow rates the following material balance equations can be written:

$$\frac{dS}{dt} = -q_f x_f + D(S_0 - S) \qquad (8)$$

$$\frac{dA}{dt} = -q_e x_e - q_m(x_{m,1} + x_{m,2}) + D(A_0 - A) + Y_{COD}q_f x_f \qquad (9)$$

$$\frac{dx_f}{dt} = \mu_f x_f - K_{d,f} x_f - \alpha_1 x_f \qquad (10)$$

$$\frac{dx_{m,1}}{dt} = \mu_m x_{m,1} - K_{d,m} x_{m,1} - \alpha_1 x_{m,1} \qquad (11)$$

$$\frac{dx_e}{dt} = \mu_e x_e - K_{d,e} x_e - \alpha_2 x_e \qquad (12)$$

$$\frac{dx_{m,2}}{dt} = \mu_m x_{m,2} - K_{d,m} x_{m,2} - \alpha_2 x_{m,2} \qquad (13)$$

$$\frac{dx_h}{dt} = \mu_h x_h - K_{d,h} x_h - \alpha_3 x_h \qquad (14)$$

where S_0, and S are the organic substrate concentration in the influent and in the anodic compartment, respectively [mg-S L^{-1}]; A_0, and A are the acetate concentration in the influent and in the anodic compartment, respectively [mg-A L^{-1}]; x_f and $x_{m,1}$ are the concentrations of fermentative and acetoclastic methanogenic microorganisms, respectively, in Layer 1 [mg-x L^{-1}]; $x_{m,2}$ and x_e, are the concentrations of acetoclastic methanogenic and electricigenic microorganisms, respectively, in biofilm Layer 2 [mg-x L^{-1}]; x_h is the concentration of hydrogenotrophic methanogenic microorganisms in biofilm Layer 3 [mg-x L^{-1}]; t is the time [d]; q_f, q_e, and q_m are the substrate consumption rates by fermentative, electricigenic, and acetoclastic methanogenic microorganisms, respectively [mg-S mg-x^{-1} d^{-1} or mg-A mg-x^{-1} d^{-1}]; μ_f, μ_m, μ_e, and μ_h are the growth rates [d^{-1}]; D is the dilution rate [$D = F_{in} V^{-1}$], F_{in} is the flow [L d^{-1}], V is the anodic compartment volume [L]; $K_{d,f}$, $K_{d,m}$, $K_{d,e}$, and $K_{d,h}$ are the microbial decay rates [d^{-1}]; Y_{COD} is the acetate yield from organic substrate [mg-S mg-A^{-1}]; and α is the dimensionless biofilm retention constant.

The biofilm retention in the anodic compartment is described by assuming that biomass growth in each biofilm layer is limited by the maximum attainable biomass concentration (X_{max}) and that the biofilm approaches its steady state thickness in the stationary phase.[25,26] Therefore, in the growth phase no biofilm washout occurs so that a batch reactor balance is used. When biofilm reaches its maximum biomass concentration a CSTR reactor balance is used. These processes are described using the biofilm retention constants α defined as:

$$\alpha_k = \begin{cases} \sum \dfrac{(\mu_\lambda x_\lambda - K_{d,\lambda} x_\lambda)}{\sum x_\lambda}, & \text{if } \left(\sum x_\lambda\right)_k \geq X_{max,k} \\ 0, & \text{otherwise} \end{cases} \qquad (15)$$

where $X_{max,k}$ is the maximum attainable biomass concentration of the k-th layer (1, 2, or 3) [mg-x L^{-1}]; and x_λ indicates each population present in the k-th layer. For layer 1, $\lambda = f, m_1$, for layer 2, $\lambda = e, m_2$, and for layer 3, $\lambda = h$.

The methane production rate in the anode compartment ($Q_{CH4,A}$ expressed in mL-CH$_4$ d^{-1}) corresponding to biofilm Layers 1, 2 and the methane production rate from H$_2$ in Layer 3 ($Q_{CH4,C}$) is described by

$$Q_{CH4,A} = Y_{CH4}q_m(x_{m,1} + x_{m,2})V \qquad (16)$$

$$Q_{CH4,C} = Y_{H2/CH4}Y_h\mu_h x_h V \qquad (17)$$

The hydrogen production rate (in mL-H$_2$ d^{-1}) is described by

$$Q_{H2} = Y_{H2}\left(\frac{I_{MEC}}{mF}\frac{RT}{P}\right) - Y_h\mu_h x_h V \qquad (18)$$

where Y_{CH4} is the methane yield [mL-CH$_4$ mg-A^{-1}]; Y_{H2} is the dimensionless cathode efficiency; $Y_{H2/CH4}$ is the yield of methane from hydrogen [mL-CH$_4$ mL-H$_2^{-1}$]; Y_h is the yield rate for hydrogen consuming methanogenic microorganisms [mL-H$_2$ mg-x^{-1}]; F is the Faraday constant [A d mol-e^{-1}]; R is the ideal gas constant [mL-H$_2$ atm K^{-1} mol-H$_2^{-1}$]; P is the anode compartment pressure [atm]; T is the MEC temperature [K]; and m is the number of electrons transferred per mol of hydrogen [mol-e^- mol-H$_2^{-1}$].

Intracellular Material Balances. The following balance equations can be written for each electricigenic microorganism:[5]

$$M_{Total} = M_{red} + M_{ox} \tag{19}$$

$$\frac{dM_{ox}}{dt} = -Y_M q_e + \frac{\gamma}{V x_e} \frac{I_{MEC}}{mF} \tag{20}$$

where M_{ox} is the oxidized mediator fraction per electricigenic microorganism [mg-M mg-x^{-1}]; M_{red} is the reduced mediator fraction per electricigenic microorganism [mg-M mg-x^{-1}]; M_{Total} is the total mediator fraction per microorganism [mg-M mg-x^{-1}]; Y_M is the oxidized mediator yield [mg-M mg-A^{-1}]; γ is the mediator molar mass [mg-M mol-M^{-1}]; and m is the number of electrons transferred per mol of mediator [mol-e^- mol-M^{-1}].

Kinetic Equations. By using multiplicative Monod kinetics[5] the following equations can be written:

$$\mu_f = \mu_{max,f} \frac{S}{K_{S,f} + S} \tag{21}$$

$$\mu_e = \mu_{max,e} \frac{A}{K_{A,e} + A} \frac{M_{ox}}{K_M + M_{ox}} \tag{22}$$

$$\mu_m = \mu_{max,m} \frac{A}{K_{A,m} + A} \tag{23}$$

$$q_f = q_{max,f} \frac{S}{K_{S,f} + S} \tag{24}$$

$$q_e = q_{max,e} \frac{A}{K_{A,e} + A} \frac{M_{ox}}{K_M + M_{ox}} \tag{25}$$

$$q_m = q_{max,m} \frac{A}{K_{A,m} + A} \tag{26}$$

where μ_{max} is the maximum growth rate [d^{-1}]; q_{max} is the maximum substrate consumption rate [mg-S mg-x^{-1} d^{-1} or mg-A mg-x^{-1} d^{-1}]; and K is the half-rate (Monod) constant [mg-S L^{-1} or mg-A L^{-1} or mg-M L^{-1}].

The growth of the hydrogenotrophic methanogens in biofilm Layer 3 (Figure 1) was assumed to depend on the H$_2$ concentration in water. Considering the low solubility of H$_2$ in water (approximately 1.5 mg L^{-1} at 30 °C[27]) and close proximity of the biofilm Layer 3 to the cathode, a zero-order growth kinetics was assumed. When no H$_2$ was produced (i.e., at a zero current), the concentration of dissolved H$_2$ was assumed to rapidly decline to zero leading to no growth. This dependence can be represented by:

$$\mu_h \begin{cases} \mu_{max,h} & \text{if } I_{MEC} > 0 \\ 0 & \text{if } I_{MEC} = 0 \end{cases} \tag{27}$$

where $\mu_{max,h}$ is the maximum growth rate of the hydrogenotrophic microorganisms [d^{-1}].

Electrochemical Equations. MEC voltage can be calculated using theoretical values of electrode potentials by subtracting ohmic, activation, and concentration losses. Therefore the following electrochemical balance can be written[28]

$$-E_{applied} = E_{CEF} - \eta_{ohm} - \eta_{conc} - \eta_{act} \tag{28}$$

where E_{CEF} represents the counter-electromotive force for the MEC [V]; η_{ohm} is the ohmic overpotential [V]; η_{conc} is the concentration overpotential [V]; η_{act} is the activation overpotential [V].

Ohm's law can be applied in eq 28 to compute ohmic losses ($\eta_{ohm} = I_{MEC} R_{int}$). Concentration losses can be divided between anode ($\eta_{conc,A}$) and cathode ($\eta_{conc,C}$) reactant mass transfer processes. Here, concentration losses at the cathode will be neglected due to the small size of H$_2$ molecules resulting in a large diffusion coefficient of H$_2$ in a gas diffusion electrode used as a cathode. The concentration losses at the anode can be calculated using the Nernst equation.[5]

$$\eta_{conc,A} = \frac{RT}{mF} \ln\left(\frac{M_{Total}}{M_{red}}\right) \tag{29}$$

Furthermore, activation losses due to slow reaction kinetics can also be separated between the anode ($\eta_{act,A}$) and cathode ($\eta_{act,C}$). Because MECs operate at high overpotential at the cathode,[2] the $\eta_{act,A}$ were assumed to be much smaller than $\eta_{act,C}$ and were neglected. The cathodic activation losses can be calculated by the Butler–Volmer equation. Assuming that the reduction and oxidation transfer coefficients that express the activation barrier symmetry are identical, the Butler–Volmer equation can be approximated as suggested by Noren and Hoffman:[29]

$$\eta_{act,C} = \frac{RT}{\beta mF} \sinh^{-1}\left(\frac{I_{MEC}}{A_{sur,A} i_0}\right) \tag{30}$$

where i_0 is the exchange current density in reference conditions [A m$^{2-1}$]; $A_{sur,A}$ is the anode surface area [m^2]; and β is either the reduction or the oxidation transfer coefficient.

Therefore, the MEC current can be calculated by combining eqs 28–30:

$$I_{MEC} = \frac{E_{CEF} + E_{applied} - \frac{RT}{mF} \ln\left(\frac{M_{Total}}{M_{red}}\right) - \eta_{act,C}}{R_{int}} \tag{31}$$

Due to the activation losses at the cathode, the I_{MEC} calculation requires a numerical solution of the nonlinear eq 31 as $\eta_{act,C} = f(I_{MEC})$. Because the solution of eq 31 could result in negative I_{MEC} values if $E_{applied}$ is smaller than the sum of η_{act}, η_{conc}, and E_{CEF}, only non-negative values of I_{MEC} were considered.

To improve model accuracy during the start-up period the R_{int} values were linked to the concentration of electricigenic microorganisms:[5]

$$R_{int} = R_{min} + (R_{max} - R_{min})e^{-K_R x_e} \tag{32}$$

where R_{MIN} is the lowest observed internal resistance [Ω], R_{MAX} is the highest observed internal resistance (at startup) [Ω], and K_R is the constant, which determines the curve steepness [L mg-x^{-1}].

■ RESULTS AND DISCUSSION

Parameter Estimation. In spite of a number of simplifying assumptions used in model formulation, the dynamic model presented above includes 36 parameters, which had to be estimated for the numerical solution of the model. The task of parameter estimation was solved by problem decomposition. First, values were assigned to physical constants (Table A in
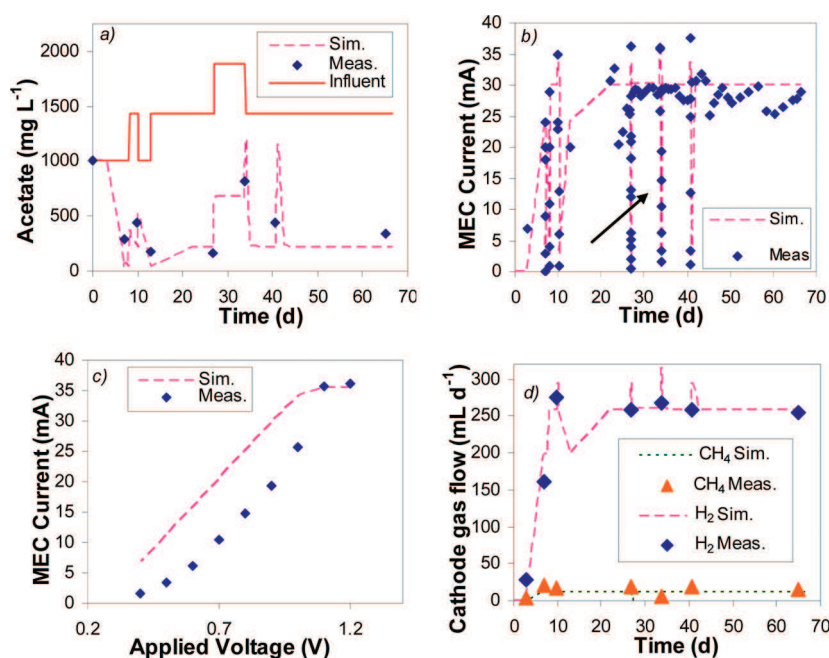
5042

dx.doi.org/10.1021/es104268g |Environ. Sci. Technol. 2011, 45, 5039–5046

Figure 2. Comparison of model outputs with experimentally measured values in MEC-1 fed with acetate: (a) acetate, (b) current, and (d) gas production in the cathode compartment. Panel c presents a detailed plot of MEC current vs voltage during the voltage scan at day 33.9 (indicated by an arrow in panel b).

Supporting Information). Next, kinetic and stoichiometric parameters estimated by Pinto et al.[5] for a MFC fed with acetate were adopted as initial values and then adjusted using experimental results obtained during MEC operation with acetate (MEC-1 test). Model parameters related to fermentative microorganisms were first adopted from ADM1[13] and then adjusted using experimental results obtained during the MEC-2 test, where sWW was used as a carbon source .

In the MEC-1 test only some model parameters could be estimated with acceptable accuracy since the measurable state variables were limited to the measurements of current, hydrogen and methane production, and acetate concentration in the effluent. After analyzing the Fisher information matrix (FIM), the maximal substrate consumption rate ($q_{max,e}$), yield (Y_M), and counter-electromotive force (E_{CEF}) were considered to be identifiable. The confidence intervals (95% confidence level) of these parameters were found to be 9.7%, 6.9%, and 4.2%, respectively.

Because current measurements were most accurate, the weight constants (w_i) required for the parameter estimation procedure (eq 1) were selected to provide higher weight to current measurements (Table B in Supporting Information). A lower weight constant was assigned to the acetate values because of significant standard deviation of these measurements. The lowest w_i values were assigned to the gas measurements because of the low accuracy of the bubble counter system for measuring gas flow rates. The resulting values of model parameters are given in Supporting Information (Table A). As mentioned above, the nonidentifiable model parameters were chosen based on Pinto et al.[5] and Batstone et al.[13]

Figure 2 presents a comparison of model outputs with the experimental results obtained in MEC-1. It should be noted that since in this test acetate was used as a carbon source, the fermentative activity was not simulated ($x_f = 0$). Furthermore, because the test was carried out in a MEC that was in operation

for over one month prior to the test startup, initial conditions for biomass density were set close to the maximum attainable biomass density (e.g., $x_h \approx X_{max,h}$). Methane production in the anodic compartment was not observed, apparently because the acetoclastic methanogens were already apparently-competed by the electricigenic microorganisms during MEC operation preceding the test.[30,31]

The simulation required less than 30 s on a PC with 2.99 GHz dual core processor. An acceptable agreement was obtained between measured and predicted effluent acetate (Figure 2a), current (Figure 2b), and gas production (Figure 2d) values. Further confirmation of the model capacity to describe process dynamics can be seen from the comparison of model outputs and experimentally measured values of current during one of the voltage scans, as shown in Figure 2c.

Once model parameters related to the electricigenic microorganisms were estimated, the MEC-2 data set was used to estimate kinetic and stoichiometric parameters of the fermentative and acetoclastic methanogenic microorganisms. Once again the FIM was used to select identifiable parameters based on the acceptable interval of confidence. The following parameters were selected for the parameter estimation procedure (notations are provided in Supporting Information, Table A): $q_{max,f}$, $q_{max,m}$, E_{CEF}, and Y_{COD}. The respective confidence intervals were 11.8%, 35.4%, 19.0%, and 18.9%. The counter electromotive force (E_{CEF}) was re-estimated because this parameter is related to the cathode potential, which can vary from electrode to electrode.

In the MEC-2 test, the measurable state variables included the values of current, sCOD and acetate concentration in the effluent, as well as the measurements of H_2 and methane production in the anode and H_2 collection compartments. The values of model parameters obtained after the parameter estimation procedure are given in Supporting Information (Table A). The estimated values of $q_{max,f}$ and $q_{max,m}$ were within the range of
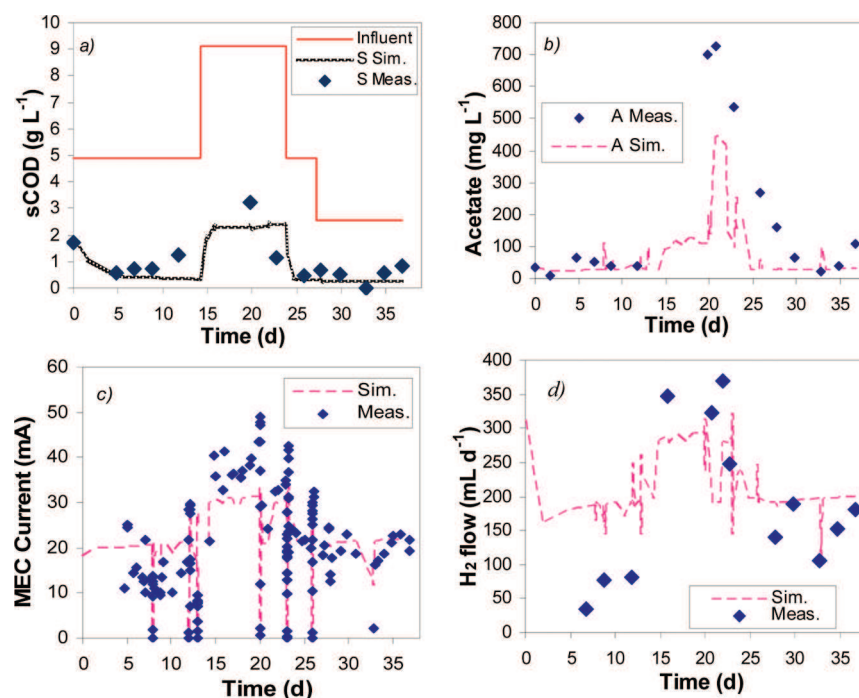
Figure 3. Comparison of model outputs with experimentally measured values in MEC-2 fed with sWW: (a) sCOD, (b) acetate, (c) current, (d) H_2 production.

Table 1. Comparison of R^2 Values Calculated for the MEC Data Sets Used for Parameters Estimation and Model Validation

state variable	MEC-1	MEC-2	MEC-3
effluent sCOD	n/a[a]	0.69	0.65
effluent VFA	0.73	0.64	0.70
current	0.82	0.78	0.82
H_2 flow-Cathode	0.85	0.85	0.65
CH_4 flow-Cathode	0.70	0.83	0.81
CH_4 flow-Anode	n/a	0.66	0.57

[a] n/a, not available.

parameters used in ADM1.[13] Also, the E_{CEF} values estimated for MEC-1 and MEC-2 were close to the values reported in the literature.[1]

Figure 3 presents a comparison of model predictions with the measurable state variables in the MEC-2 test. Acetate and sCOD model outputs generally follow experimental measurements, although a certain underestimation can be seen. Nevertheless, this underestimation was acceptable considering the larger standard deviations of sCOD and acetate measurements in comparison to I_{MEC} measurements. Model predictions of I_{MEC} closely followed the measured values for most of the tested sWW loads with the exception of the highest load, when I_{MEC} values were underestimated (Figure 3c). Gas flow measurements were followed reasonably well (Figure 3d) in spite of the large fluctuations in measured H_2 flow. Once again, voltage scans led to short-term drops in H_2 production during the first part of each voltage scan when the applied voltage was low.

A statistical measure of the model accuracy was provided by calculating the adjusted coefficients of determination (R^2) of model outputs. R^2 values calculated both for MEC-1 and MEC-2 data sets are provided in Table 1. Regardless of the low weight

constants assigned to H_2 measurements, the R^2 values corresponding to H_2 measurements were above 0.8 because H_2 production was directly proportional to current (eq 18) and the current measurements were followed quite well by the model as can be seen from Figures 2b and 3c. Overall, R^2 calculations confirmed a reasonable agreement between experimentally measured and calculated state variables.

Model Validation. Model validation was carried out using the results obtained in MEC-3, which was fed with sWW. Notably, the organic load profiles in MEC-2 and MEC-3 tests were different (Figures 3a and 4a), thus eliminating any possible correlation between the two data sets. During the model validation procedure, all model parameters were kept unchanged apart from the internal resistance value (R_{MIN} in Supporting Information), which was re-estimated using the voltage scan technique[17,32] and was found to be higher (35 Ω vs 20 Ω) than in the MEC-2 test.

Figure 4 presents a comparison between the predicted and measured state variables in the MEC-3 test. A satisfactory agreement was obtained, especially between predicted and measured values of current and H_2 flow (Figure 4c and d), but also for sCOD and acetate values (Figure 4a and b). R^2 calculations (Table 1) confirmed acceptable accuracy of model predictions. Importantly, similar R^2 values were obtained for both MEC-2 (parameter estimation) and MEC-3 (model validation) data sets, which confirmed the predictive capacity of the model.

Model Analysis. In this section we demonstrate an application of the multi-population model described above for predicting H_2 production and COD removal in a MEC operated at various applied voltages and influent COD concentrations. The model analysis presented in this section is performed by integrating model eqs 8−32 for a period of 200 days and analyzing MEC performance at the end of this period, i.e., steady state analysis is presented.
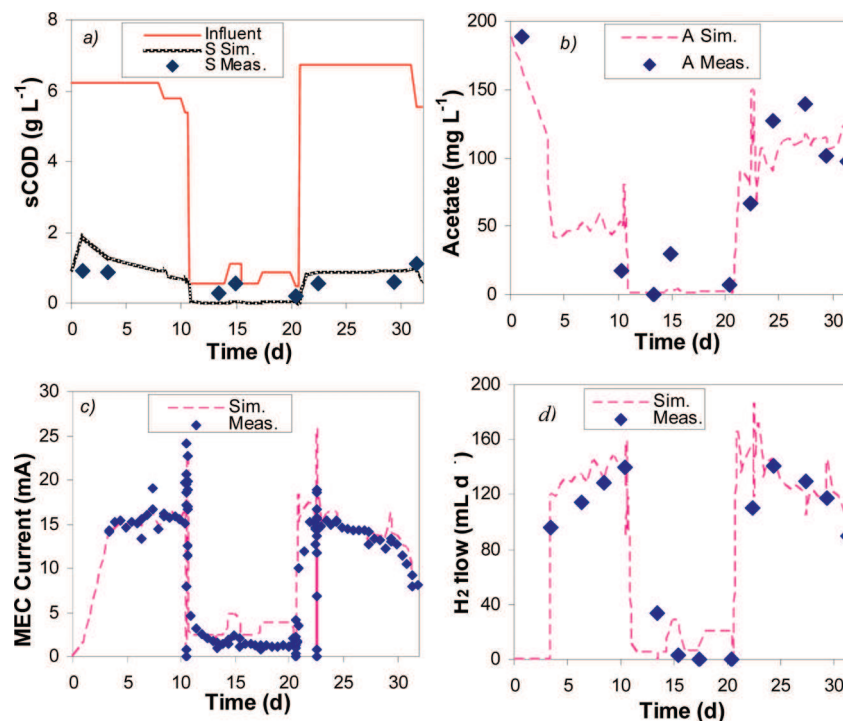
Figure 4. Model validation based on the experimental results obtained with sWW-fed MEC-3 (a) sCOD, (b) acetate, (c) current, (d) H_2 production.
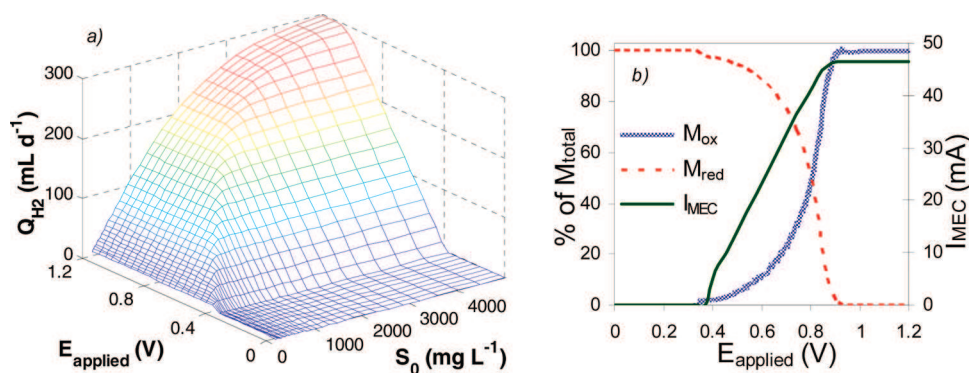

Figure 5. Predicted dependency of H_2 production on applied voltage and influent COD concentration (a). The predicted changes in mediator concentrations are shown in panel b. Additional graphs are provided in Supporting Information.

Figure 5a shows the effect of applied voltage and influent COD concentrations on H_2 production. As expected, H_2 production is maximized at the highest applied voltage of 1.2 V. This prediction agrees with both the previously reported results[1,2] and the experiments described above. Analysis of eq 31 shows that no current can be produced at applied voltages below the sum of η_{act}, η_{conc}, and E_{CEF}. Above this threshold the electricigenic microorganisms are able to transfer the electrons to the anode resulting in a measurable current and H_2 production. The dependence of I_{MEC} on applied voltage is further illustrated in Figure 5b, which shows the predicted levels of oxidized (M_{ox}) and reduced (M_{red}) forms of the intracellular mediator. As the applied voltage increases, the concentration of M_{ox} augments until it reaches its maximum value equal to M_{Total}. Since I_{MEC} is dependent on M_{ox}, it also increases. Once the maximum M_{ox} concentration is reached, no further increase in I_{MEC} can be achieved even if the applied voltage is increased. It should be

mentioned that MEC operation at excessively high applied voltages results in energy losses and might lead to the onset of water electrolysis at around 1.8 V.[1]

Model predictions in Figure 5a also demonstrate the effect of influent COD concentration and suggest that the high rates of H_2 production require a sufficient organic load. This can be related to the Monod kinetics of the fermentative microorganisms (eq 24). At low COD concentrations less acetate is produced. The shortage of acetate for the electricigenic microorganisms results in lower current and therefore in a reduced H_2 flow. Additional model analysis is provided in Supporting Information.

To conclude, the multipopulation model presented above provides a useful guidance regarding MEC design and operation. Also, the model simplicity makes it suitable for real-time process control, where timely adjustment of operational parameters could be used for maximizing hydrogen production while achieving the required degree of COD removal.

■ ASSOCIATED CONTENT

ⓢ Supporting Information. Model analysis, additional figures and tables. This material is available free of charge via the Internet at http://pubs.acs.org.

■ AUTHOR INFORMATION

Corresponding Author

*Phone:1-514-496-2664; fax:1-514-496-6265; e-mail: Boris.Tartakovsky@nrc-cnrc.gc.ca.

■ ACKNOWLEDGMENT

■ REFERENCES

(1) Rozendal, R. A.; Hamelers, H. V. M.; Euverink, G. J. W.; Metz, S. J.; Buisman, C. J. N. Principle and perspectives of hydrogen production through biocatalyzed electrolysis. *Int. J. Hydrogen Energy* **2006**, *31* (12), 1632–1640.

(2) Logan, B. E.; Call, D.; Cheng, S.; Hamelers, H. V. M.; Sleutels, T. H. J. A.; Jeremiasse, A. W.; Rozendal, R. A. Microbial Electrolysis Cells for High Yield Hydrogen Gas Production from Organic Matter. *Environ. Sci. Technol.* **2008**, *42* (23), 8630–8640.

(3) Logan, B. E.; Hamelers, B.; Rozendal, R. A.; Schroder, U.; Keller, J.; Freguia, S.; Aelterman, P.; Verstraete, W.; Rabaey, K. Microbial Fuel Cells: Methodology and Technology. *Environ. Sci. Technol.* **2006**, *40* (17), 5181–5192.

(4) Rozendal, R. A.; Hamelers, H. V. M.; Rabaey, K.; Keller, J.; Buisman, C. J. N. Towards practical implementation of bioelectrochemical wastewater treatment. *Trends Biotechnol.* **2008**, No. 26, 450–459.

(5) Pinto, R. P.; Srinivasan, B.; Manuel, M. F.; Tartakovsky, B. A two-population bio-electrochemical model of a microbial fuel cell. *Bioresour. Technol.* **2010**, *101* (14), 5256–5265.

(6) Marcus, A. K.; Torres, C. I.; Rittmann, B. E. Conduction-based modeling of the biofilm anode of a microbial fuel cell. *Biotechnol. Bioeng.* **2007**, *98* (6), 1171–1182.

(7) Picioreanu, C.; Head, I. M.; Katuri, K. P.; van Loosdrecht, M. C. M.; Scott, K. A computational model for biofilm-based microbial fuel cells. *Water Res.* **2007**, *41* (13), 2921–2940.

(8) Zeng, Y.; Choo, Y. F.; Kim, B.-H.; Wu, P. Modelling and simulation of two-chamber microbial fuel cell. *J. Power Sources* **2010**, *195* (1), 79–89.

(9) Picioreanu, C.; van Loosdrecht, M. C. M.; Curtis, T. P.; Scott, K. Model based evaluation of the effect of pH and electrode geometry on microbial fuel cell performance. *Bioelectrochemistry* **2010**, *78*, 8–24.

(10) Marcus, A. K.; Torres, C. I.; Rittmann, B. E. Analysis of a microbial electrochemical cell using the proton condition in biofilm (PCBIOFILM) model. *Bioresour. Technol.* **2010**, *102* (1), 253–262.

(11) Picioreanu, C.; Katuri, K. P.; Head, I. M.; Van Loosdrecht, M. C. M.; Scott, K. Mathematical model for microbial fuel cells with anodic biofilms and anaerobic digestion. *Water Sci. Technol.* **2008**, *57* (7), 965–971.

(12) Bernard, O.; Hadj-Sadok, Z.; Dochain, D.; Genovesi, A.; Steyer, J.-P. Dynamical model development and parameter identification for an anaerobic wastewater treatment process. *Biotechnol. Bioeng.* **2001**, *75* (4), 424–438.

(13) Batstone, D. J.; Keller, J.; Angelidaki, I.; Kalyuzhnyi, S. V.; Pavlostathis, S. G.; Rozzi, A.; Sanders, W. T. M.; Siegrist, H.; Vavilin, V. *Anaerobic Digestion Model No 1 (ADM1)*; IWA Publishing: London, UK, 2002.

(14) Moletta, R.; Verrier, D.; Albagnac, G. Dynamic modelling of anaerobic digestion. *Water Res.* **1986**, *20* (4), 427–434.

(15) APHA. *Standard Methods for the Examination of Water and Wastewater*, 19th ed.; American Public Health Association: Washington, DC, 1995.

(16) Tartakovsky, B.; Manuel, M. F.; Neburchilov, V.; Wang, H.; Guiot, S. R. Biocatalyzed hydrogen production in a continuous flow microbial fuel cell with a gas phase cathode. *J. Power Sources* **2008**, *182* (1), 291–7.

(17) Manuel, M.-F.; Neburchilov, V.; Wang, H.; Guiot, S. R.; Tartakovsky, B. Hydrogen production in a microbial electrolysis cell with nickel-based gas diffusion cathodes. *J. Power Sources* **2010**, *195* (17), 5514–5519.

(18) Nelder, J. A.; Mead, R. A Simplex Method for Function Minimization. *Comput. J.* **1965**, *7* (4), 308–313.

(19) Lettinga, G. Anaerobic digestion and wastewater treatment systems. *Antonie van Leeuwenhoek* **1995**, *67*, 3–28.

(20) Jeyaseelan, S. A simple mathematical model for anaerobic digestion process. *Water Sci. Technol.* **1997**, *35*, 185–191.

(21) Hu, H.; Fan, Y.; Liu, H. Hydrogen production using single-chamber membrane-free microbial electrolysis cells. *Water Res.* **2008**, *42* (15), 4172–4178.

(22) Wang, A.; Liu, W.; Cheng, S.; Xing, D.; Zhou, J.; Logan, B. E. Source of methane and methods to control its formation in single chamber microbial electrolysis cells. *Int. J. Hydrogen Energy* **2009**, *34* (9), 3653–3658.

(23) Yang, Y.; Tsukahara, K.; Sawayama, S.; Maekawa, T. Anaerobic digestion by a fixed and fluidized hybrid reactor packed with carbon felt. *Mater. Sci. Eng., C* **2004**, *24*, 893–899.

(24) Rauch, W.; Vanhooren, H.; Vanrolleghem, P. A. A simplified mixed-culture biofilm model. *Water Res.* **1999**, *33* (9), 2148–2162.

(25) Mu, S. J.; Zeng, Y.; Wu, P.; Lou, S. J.; Tartakovsky, B. Anaerobic digestion model no. 1-based distributed parameter model of an anaerobic reactor: I. Model development. *Bioresour. Technol.* **2008**, *99* (9), 3665–3675.

(26) Wanner, O.; Gujer, W. Multispecies Biofilm Model. *Biotechnol. Bioeng.* **1986**, *28* (3), 314–328.

(27) Sander, R. Compilation of Henry's Law Constants for Inorganic and Organic Species of Potential Importance in Environmental Chemistry (Version 3), 1999. http://www.henrys-law.org.

(28) *Fuel Cell Handbook 2005*; National Energy Technology Laboratory, U.S. Department of Energy and University Press of the Pacific, 2005.

(29) Noren, D. A.; Hoffman, M. A. Clarifying the Butler-Volmer equation and related approximations for calculating activation losses in solid oxide fuel cell models. *J. Power Sources* **2005**, *152* (1−2), 175–181.

(30) Pinto, R. P.; Tartakovsky, B.; Perrier, M.; Srinivasan, B. Optimizing Treatment Performance of Microbial Fuel Cells by Reactor Staging. *Ind. Eng. Chem. Res.* **2010**, *49* (19), 9222–9229.

(31) Pinto, R. P.; Srinivasan, B.; Guiot, S. R.; Tartakovsky, B. The Effect of Real-Time External Resistance Optimization on Microbial Fuel Cell Performance. *Water Res.* **2011**, *45* (4), 1571–1578.

(32) Hrapovic, S.; Manuel, M. F.; Luong, J. H. T.; Guiot, S. R.; Tartakovsky, B. Electrodeposition of nickel particles on a gas diffusion cathode for hydrogen production in a microbial electrolysis cell. *Int. J. Hydrogen Energy* **2010**, *35* (14), 7313–7320.